Voltage-sensor conformation shapes the intra-membrane drug binding site that determines gambierol affinity in Kv channels

*Title page

Voltage-sensor conformation shapes the intra-membrane drug binding site that determines gambierol affinity in Kv channels.

Authors: Ivan Kopljar[1Ψ], Alessandro Grottesi[2], Tessa de Block[1], Jon D. Rainier[3], Jan Tytgat[4], Alain J. Labro[1], Dirk J. Snyders[1]*

Affiliations:

[1]Laboratory for Molecular Biophysics, Physiology and Pharmacology, University of Antwerp, 2610 Antwerp, Belgium

[2]CINECA – Sede di Roma – Via dei Tizii 6, 00185 – Rome, Italy

[3]Department of Chemistry, University of Utah, Salt Lake City, UT 84112-0850, USA

[4]Toxicology and Pharmacology, University of Leuven Campus Gasthuisberg, 3000 Leuven, Belgium

[Ψ]Current affilation: Global Safety Pharmacology, PD&S, Discovery Sciences, Janssen Research and Development, Beerse, Belgium

***Corresponding Author:**

Dirk J. Snyders, M.D., Ph.D.
Laboratory for Molecular Biophysics, Physiology and Pharmacology
Department of Biomedical Sciences
University of Antwerp
Universiteitsplein 1, T5.35
2610 Antwerp, Belgium
Phone: +32-(3)-820-2335
Fax: +32-(3)-820-2326
Email: dirk.snyders@uantwerpen.be

Abstract

Marine ladder-shaped polyether toxins are implicated in neurological symptoms of fish-borne food poisonings. The toxin gambierol, produced by the marine dinoflagellate *Gambierdiscus toxicus*, belongs to the group of ladder-shaped polyether toxins and inhibits Kv3.1 channels with nanomolar affinity through a mechanism of gating modification. Binding determinants for gambierol localize at the lipid-exposed interface of the pore forming S5 and S6 segments, suggesting that gambierol binds outside of the permeation pathway. To explore a possible involvement of the voltage-sensing domain (VSD), we made different chimeric channels between Kv3.1 and Kv2.1, exchanging distinct parts of the gating machinery. Our results showed that neither the electro-mechanical coupling nor the S1-S3a region of the VSD affect gambierol sensitivity. In contrast, the S3b-S4 part of the VSD (paddle motif) decreased gambierol sensitivity in Kv3.1 more than 100-fold. Structure determination by homology modeling indicated that the position of the S3b-S4 paddle and its primary structure defines the shape and\or the accessibility of the binding site for gambierol, explaining the observed differences in gambierol affinity between the channel chimeras. Furthermore, these findings explain the observed difference in gambierol affinity for the closed and open channel configurations of Kv3.1, opening new possibilities for exploring the VSDs as selectivity determinants in drug design.

Key words

voltage-gated potassium channel - electrophysiology - gating modifier - polycyclic ether toxin - ciguatoxins

Introduction

Voltage-gated potassium (Kv) channels are membrane-imbedded proteins that function as key regulators of the electrical signaling in biological systems. They share a tetrameric architecture formed by α-subunits, each containing six transmembrane α-helical segments (S1-S6) (Long et al., 2005). The S5-S6 segments co-assemble with fourfold symmetry into the central K^+ conducting pore that is surrounded by four voltage-sensing domains (VSDs) composed of S1-S4. Conformational changes in the VSDs are transmitted to the channel gate in the bottom part of S6 (S6c) via the S4-S5 linker, controlling ion permeation (Blunck and Batulan, 2012; Labro and Snyders, 2012; Lu et al., 2002). Natural toxins and pharmacological compounds are known to target these K_v channels through several distinct binding sites, mainly located in the pore domain or the VSDs (Wulff et al., 2009).

Gambierol, which is produced by the marine dinoflagellate *Gambierdiscus toxicus*, belongs to the group of ladder-shaped polyether toxins (Satake et al., 1993). Gambierol shares its chemical structure with that of the ciguatoxins and brevetoxins, which are site 5 modulators of voltage-gated sodium (Nav) channels (Catterall et al., 2007; Nicholson and Lewis, 2006), but some members inhibit Kv channels as well (Birinyi-Strachan et al., 2005; Hidalgo et al., 2002; Mattei et al., 2010; Schlumberger et al., 2010a). Gambierol does not affect Nav channels, but has been shown to be a potent inhibitor of Kv channels (Cuypers et al., 2008; Ghiaroni et al., 2005; Perez et al., 2012; Schlumberger et al., 2010b), and specifically of Kv3.1 (Kopljar et al., 2009). Several of these polyether toxins (e.g. ciguatoxins) cause ciguatera fish poisoning in humans, characterized by neurological and gastrointestinal symptoms (Nicholson and Lewis, 2006). Gambierol has been shown to induce neurological symptoms in mice (Fuwa et al., 2004) and to augment spontaneous Ca^{2+} oscillations in cerebrocortical neurons as a consequence of Kv channel inhibition (Cao et al., 2014).

The binding site of gambierol is located outside the permeation pathway at a lipid-accessible inter-subunit space between the VSD and the pore domain, with binding determinants in both the S5 and S6 segment (Kopljar et al., 2009). This binding site resembles that of the Psora-4 compound which bind at so called side-pockets of the K^+ pore (Marzian et al., 2013). The mechanism of channel inhibition by gambierol is based on stabilizing Kv3.1 channels in their high affinity resting (closed) state (Kopljar et al., 2013). As a result, the voltage dependence

of activation is shifted by more than +120 mV to more positive potentials, preventing channel opening in the physiologically relevant voltage range. We previously showed that introducing the S6 region of Kv3.1 into the gambierol-insensitive Kv2.1 channel transferred Kv3.1´s high affinity only partially, whereas the S5 swap did not alter the affinity for gambierol significantly (Kopljar et al., 2009). We therefore anticipated that other regions besides the pore domain might contribute to the mechanism of gating modification by gambierol. By constructing chimeric channels between Kv3.1 and Kv2.1, we show that the S3b-S4 section of the VSD, but not its S1-S3a region nor the electromechanical coupling, alters the sensitivity for gambierol. Furthermore, we used homology modelling to obtain structures for the closed and open conformation of Kv3.1. In these models, we observed VSD-dependent changes of the shape of the pocket between the VSD and the pore (referred throughout the manuscript as gambierol's binding pocket) such that in the open state the binding pocket is partially obliterated.

Results

The VSD region modulates the affinity for gambierol

Gambierol inhibits Kv channels by modulating the gating machinery and preventing VSD movement(s) (Kopljar et al., 2013). We previously showed that T427 in the middle of S6 is an important determinant for the high affinity of Kv3.1. In Kv2.1, a valine is present at the corresponding location (Kopljar et al., 2009). To identify parts of the gating machinery that might modulate the gambierol sensitivity, we designed several chimeric channels taking advantage of the difference in affinity between Kv2.1 (low) and Kv3.1 (high). To this end, the electro-mechanical coupling between the VSD and the channel gate (S4-S5 linker and S6c segments), and the VSD (S1-S4, S1-S3a and the S3b-S4 region) were in Kv2.1 replaced individually by the corresponding Kv3.1 sequence (Fig.1). Transfer of the S4-S5 linker and S6c segment (Electro-Mechanical coupling) resulted in the Kv3.1_EMcoupling_2.1 chimera that yielded functional channels (Figure 2A). These Kv3.1_EMcoupling _2.1 channels were inhibited by gambierol (Figure 2A-B) with an IC_{50} value of 2.4 ± 0.2 nM (n = 3), which was similar to the affinity of WT Kv3.1 channels (IC_{50} = 1.2 nM). Thus the EM-coupling of Kv2.1 is functional in the Kv3.1 background, but does not reduce the high affinity.

Next, we investigated the contribution of the VSD and exchanged the entire S1-S4 section of Kv3.1 by the corresponding Kv2.1 sequence. This exchange resulted in functional channels that, in contrast to the electro-mechanical coupling chimera, displayed a reduced gambierol affinity (IC_{50} value of 280 ± 40 nM, n = 4). Swartz and co-workers previously showed that the S3b-S4 region, a VSD segment that has been identified as the voltage-sensor paddle, is transportable between voltage-gated ion channels (Alabi et al., 2007). Therefore, to determine the VSD region involved in gambierol sensitivity we exchanged the S1-S3a and S3b-S4 region separately. Substituting the S3b-S4 region by Kv2.1 sequence generated the Kv3.1_S3b-S4_2.1 chimera, which displayed a reduced gambierol affinity (IC_{50} value of 143 ± 28 nM, n = 4) similar to the S1-S4 chimera. On the other hand, gambierol inhibited the Kv3.1_S1-S3a_2.1 chimera with high affinity, displaying an IC_{50} value of 1.9 ± 0.2 nM (n = 3). Collectively, these results demonstrate that neither the electromechanical coupling (S4-S5 linker with S6c) nor the proximal part of the VSD (S1-S3a) contribute to the high gambierol sensitivity in Kv3.1

channels. On the other hand, replacing in Kv3.1 the S3b-S4 region of the VSD by Kv2.1 sequence reduced gambierol affinity a 120-fold.

The VSD channel chimeras assemble properly

It is well known that mutations may change the native conformation of the channel protein, hereby affecting indirectly the interaction of the toxin/drug with its binding site through allosteric effects. Hence, it is important to differentiate direct compound-channel interactions from effects caused by overall conformational changes induced by the mutation(s). Therefore, we analyzed the biophysical properties of the chimaeras (in particular the VSD chimeras) and compared them with the WT channels. The voltage dependence of channel activation was investigated by determining the conductance versus voltage (GV) curves, which were characterized by a midpoint ($V_{1/2}$) value and slope factor (k). For the three VSD chimeras the $V_{1/2}$ was indeed shifted towards more positive potentials (Figure 3A). More importantly, all the VSD chimeras displayed similar slope factors which were comparable to the values of Kv2.1 (Table 1). This suggests that the functional properties of the VSD were transferred from Kv2.1 onto Kv3.1. The time constants of channel activation were for all VSD chimeras comparable to those of Kv3.1, when the shifted voltage dependence of channel activation was taken into account (Figure 3B). These chimeras displayed a similar shift in their voltage dependence of channel inactivation without major alterations in their overall inactivation process and all displayed a U-type inactivation profile similar to Kv2.1 (supplemental Figure S1). Thus, except a shifted voltage dependence of activation and inactivation, all VSD chimeras (S1-S4, S1-S3a and S3b-S4) displayed similar biophysical properties comparable to either Kv2.1 or Kv3.1.

Various studies have addressed different models for determining the energy landscape of the activation pathway from closed to a fully open (Sigg, 2014; Sigg and Bezanilla, 2003). If we assume that the GV curves are representative for voltage sensing (movement of the gating charges of the VSD), a shift in $V_{1/2}$ potential is mostly a change in the offset value with only a minor impact on the shape of the energy landscape (parallel shift of the landscape along the voltage axis). In contrast, a change in the slope factor or changes in the kinetics usually reflect a strong change in the shape energy landscape. Since structural changes determine the energy landscape (Delemotte et al., 2015), we propose that the shifted midpoint of the chimeras Kv3.1_S1-S4_2.1, Kv3.1_S1-S3a_2.1 and Kv3.1_S3b-S4_2.1 has a minimal impact on the

structure, i.e. all these VSD chimeras fold correctly and their gating machinery undergoes structural reorientations comparable to those of WT channels. Without a 3D structure this remains of course hypothetical but the supplemental figure S2 shows that there was no correlation between the channel´s sensitivity for gambierol and its $V_{1/2}$ value or slope factor. Therefore, major distortions in channel conformation are unlikely the explanation for the different affinities of the VSD chimeras for gambierol.

To investigate the structural integrity of the pore domain in the different VSD chimeras, independently of their biophysical properties, we tested their affinity (IC_{50} value) for well-established pore blockers. We tested the integrity of the external pore mouth using TEA (Heginbotham and MacKinnon, 1992), whereas for the internal cavity (pore) we used flecainide (Herrera et al., 2005). The three VSD chimeras displayed an affinity for externally applied TEA similar to that of WT Kv3.1 channels, suggesting that the conformation of the external pore mouth was preserved in the VSD chimeras (Figure 3C and supplemental Figure S3). The block of WT Kv3.1 channels and VSD chimeras by flecainide was calculated at depolarizing potentials of $V_{1/2}$ +30 mV. Flecainide displayed only minor (< 2-fold) differences in IC_{50} values between WT channels and chimaeras, indicating that also the conformation of the central cavity of the pore domain was not affected by exchanging the complete VSD or parts of it. Collectively, these results indicate that the K^+ permeation pore was preserved, suggesting that the conformation of S5 and S6 did not change significantly in the VSD chimeras compared to WT Kv3.1.

To further explore the role of the S3b-S4 paddle region, we made an opposite exchange and transferred the S3b-S4 region of Kv3.1 into the intermediate-sensitive Kv2.1 V404T mutant. This mutant contains the important threonine residue in S6 that is a key mediator of gambierol sensitivity between Kv subfamilies (Kopljar et al., 2009). Unexpectedly, the Kv2.1 V404T_S3b-S4_3.1 chimera displayed an IC_{50} of 900 ± 41 nM (n = 3, Table 1), which is ~2-fold lower than the previously reported value of the Kv2.1 V404T mutant (IC_{50} = 504 ± 28 nM, n = 3) (Kopljar et al., 2009). However, analysis of the biophysical properties showed that the voltage dependence of channel activation ($V_{1\2}$ = 109.7 ± 4.9 mV, n = 6) and the slope factor (k = 27.3 ± 3.7 mV, n = 6) of this Kv2.1 V404T_S3b-S4_3.1 chimera were significantly altered compared to WT Kv2.1 (Table 1). In contrast to the VSD chimeras discussed above, the significant shallower slope factor of the Kv2.1 V404T_S3b-S4_3.1 chimera suggested a more drastic effect on the

shape of the energy landscape that the channel traverses when going from closed to open. Hence, replacing in Kv2.1 V404T the S3b-S4 region by the Kv3.1 sequence did not increase the sensitivity for gambierol further, most likely because this chimera induced major conformational changes and presumably decreased the gambierol sensitivity via allosteric effects. Therefore, no strong conclusions can be drawn from this construct regarding gambierol sensitivity.

Kv3.1 homology models display VSD-dependent changes in gambierol´s binding pocket between the VSD and the pore.

Since the channel kinetics and affinity for well-established pore blockers of the VSD chimeras argued against major conformational changes of the channel protein, the S3b-S4 region influences gambierol sensitivity by either interacting directly with gambierol or by sculpting gambierol´s binding pocket. In the first scenario, the lipid accessible pocket that accommodates gambierol should be lined by both regions and gambierol should be able to span the distance between the S3b-S4 region and its binding determinants in the S5 and S6 segment. To determine whether gambierol´s binding pocket stretches from its binding determinant(s) in S6 until the S3b-S4 region, we built Kv3.1 homology models for both the closed and open conformation and determined the contour of gambierol´s binding pocket between the VSD and the pore domain by means of FPOCKET (see Methods). Using this approach we characterized the pocket that is lined by residue T427 in S6, which is a key determinant for gambierol sensitivity (Kopljar et al., 2009). In the model of the closed state this pocket is lined on top by the S3b-S4 region of the VSD, at the bottom by the S4-S5 linker, and sideways by parts of the S5 and S6 segments. Interestingly, this pocket has roughly an hourglass shape, with a narrower section at the center. This central constriction is 4.6 x 4.8 Å wide and 6.5 Å long. At this constriction point the estimated volume is about 143.5 $Å^3$ which is still enough to accommodate the passage of a compound like gambierol that has an estimated total volume of 130 $Å^3$ over the same length (in the typical polyether configuration). Thus, in the closed state there exists a pathway that connects residue T427 in S6 and the S3b-S4 region of the VSD. The approximate distance between S3b-S4 and T427 along this path is about 20 Å, a distance that can be spanned by gambierol (which is 25 Å long with polyether rings of 5 Å wide at the largest, therefore fitting within the relative constriction point).

Using a similar approach, we determined the pocket that is lined by residue T427 in the open state model of Kv3.1. The shape of the pocket is clearly different from that of the closed state model and the space around the S3b-S4 region gets disconnected from the one around T427 in S6. To quantify this behavior, the volume of the space that surrounds residue T427 was calculated for Kv3.1´s closed and open state model as described in the Methods section (Figure 4A-B). In agreement with the visible changes, the volume size of gambierol´s putative binding pocket was 1350 $Å^3$ in the open state model, whilst it was larger in the closed model and amounted to 1750 $Å^3$. Thus, the conformational changes of the VSD associated with channel opening also influence the shape of the binding pocket for gambierol.

VSD´s S3b-S4 sequence modulates gambierol´s binding pocket

In Kv3.1 the shape of gambierol´s binding pocket clearly changed when the channel opened; the pocket became more confined around S6c and made no connection between S3b-S4 and T427 in S6. This VSD-dependent change in gambierol´s binding pocket agreed with the experimental observation that the closed conformation is the high affinity state and that the sensitivity decreases drastically upon channel activation, even resulting in a complete dissociation of gambierol [19]. As the S3b-S4 region appeared to line gambierol´s binding pocket in the closed state model of Kv3.1, we determined the shape of this pocket in a closed and open state model for the Kv2.1 channel. Interestingly, the shape of the binding pocket was significantly different in Kv2.1 compared to Kv3.1 (Figure 4), which was initially unexpected as both the Kv2.1 and Kv3.1 models were constructed from the same template structures (see Methods). In case of Kv2.1, we calculated the pocket that was lined by the S6 residue V404, which is the counterpart of residue T427 in Kv3.1. Most interestingly, in the closed state the pocket in Kv2.1 is not lined by the S3b-S4 paddle region (Figure 4C). As a result the pocket does not connect the S3b-S4 paddle region and the S6c, as is the case in Kv3.1 in the closed (high affinity) state. In fact, the pocket of Kv2.1´s closed state resembles that of the open state of Kv3.1. Finally, in the open state of Kv2.1 the pocket is similarly confined around S6c and there is no connection with the S3b-S4 paddle (Figure 4D), as was the case in Kv3.1.

To investigate the impact of substituting the S3b-S4 paddle region in Kv3.1 by Kv2.1 sequence on the structure of gambierol´s putative binding pocket we performed similar homology modeling and determined the shape of the pocket in the closed and open state model

of the Kv3.1_S3b-S4_2.1 chimera. First, we focused on the closed state model and determined the pocket that is lined by residue T427 in S6. Interestingly, the pocket is more constricted at the center compared to the closed state model of Kv3.1. This indicates that the pocket in the Kv3.1_S3b-S4_2.1 chimera might connect both regions but it is less likely to occur compared to the Kv3.1 model (Figure 4E). Thus, the shape of the pocket in the Kv3.1_S3b-S4_2.1 chimera appears to be intermediate between those observed in the closed model of Kv3.1 and Kv2.1 (Figure 4). As was the case for Kv3.1 and Kv2.1, the pocket in the chimera is smaller and more confined around the S6c helix in the open state model (Figure 4F).

Discussion

Gambierol inhibition is modulated by the VSD but not the electromechanical coupling.

The S4-S5 linker with possible contribution of S6c (i.e., the electromechanical coupling) has been shown to be a key determinant for channel inhibition by general anesthetics such as halothane and alkanols (Barber et al., 2011; Bhattacharji et al., 2006; Harris et al., 2000). Exchanging in Kv3.1 the S4-S5 linker together with the S6c by Kv2.1 sequence did not alter the high-affinity inhibition of Kv3.1 by gambierol, which suggests that the mechanism of channel inhibition by gambierol differs from that of general anesthetics.

The VSD has been shown to be the molecular target of several gating modifying compounds such as peptide toxins from tarantula spiders that inhibit Kv channels by interacting with the S3b-S4 paddle region (Li-Smerin and Swartz, 2000; Swartz and MacKinnon, 1997). These toxins act as a cargo (load) on the VSD, stabilizing the closed state and shifting the voltage dependence of channel activation towards more depolarized potentials (Phillips et al., 2005). An opposite effect is seen with polyunsaturated fatty acids (PUFA's) that shift the voltage dependence of channel opening towards more hyperpolarized potentials by acting close to the extracellular lipid-facing parts of S3 and S4 (Borjesson and Elinder, 2011; Ottosson et al., 2014). Our results demonstrated that transplanting the complete VSD or only the S3b-S4 region of Kv2.1 into the Kv3.1 background decreased the affinity for gambierol more than a 100-fold (Figure 2). Transplanting only the proximal S1-S3a region of the VSD did not change Kv3.1´s sensitivity for gambierol. Since all three VSD chimeras displayed similar biophysical properties, the decreased gambierol sensitivity in the complete VSD and the S3b-S4 chimera is unlikely to result from allosteric effects induced by a misfolded VSD. Furthermore, all VSD chimeras remained sensitive for the pore blockers TEA and flecainide, indicating that the conformation of the pore domain was also intact. The reverse chimera, introducing the S3b-S4 region of Kv3.1 into the Kv2.1 V404T mutant, however resulted in channels with strongly altered biophysical properties (Table 1). This indicates that the folding of this Kv2.1 V404T_S3b-S4_3.1 chimera was more disrupted, and consequently the results of this chimera are not suitable for drawing conclusions regarding the binding site of gambierol. Collectively, these results suggested that the S3b-S4 region of the VSD is a molecular determinant of channel inhibition by gambierol, as is the case for gating modifier peptide toxins (Swartz, 2007).

VSD conformation modulates the membrane-accessible space that accommodates gambierol.

Gambierol has been proposed to occupy a membrane-accessible pocket between the VSD and the S5-S6 segment of the pore domain (Kopljar et al., 2009), which may be similar to the side-pockets that accommodate psora compounds (Marzian et al., 2013). The binding site for gambierol is reminiscent of the neurotoxin site 5 in Nav channels (Catterall et al., 2007; Trainer et al., 1991; Trainer et al., 1994). Interestingly, the affinity of the Nav1.4 channel for the ladder-shaped polyether toxin ciguatoxin-3C could be reduced by neutralizing a charged residue in the VSD of domain 2 (Yamaoka et al., 2011). This observation is in line with our data, suggesting that the mechanism of action of (some) polyether toxins on Nav and Kv channels is influenced by the VSD.

Gambierol inhibits the Kv3.1 channel by immobilizing VSD movement(s) upon interaction with residues of the S5 and S6 segment (Kopljar et al., 2013). One possibility is that gambierol interacts also with the VSD´s S3b-S4 region whereby it anchors the VSD to the pore domain resulting in a stabilization of the gating machinery in the resting closed state. Thus, gambierol would contact both regions simultaneously when occupying its binding pocket. Analyzing the lipid accessible pocket between the VSD and the pore domain of neighboring subunits illustrated that this pocket forms a pathway between the S3b-S4 region of the VSD and residue T427 in S6 when the Kv3.1 channel is closed (Fig. 4A). Furthermore, both regions appeared sufficiently close together for gambierol to span the distance and interact with both domains simultaneously. Primary sequence alignment showed that the sequence of the S3-S4 linker is indeed conserved within the Kv3 subfamily (supplemental Figure S3). However, this is not the situation in the Kv1 subfamily and the S3-S4 linker of Kv1.1, Kv1.2, Kv1.3, Kv1.4 and Kv1.5 is highly variable in both length and sequence although all channels showed a similar affinity for gambierol (Cuypers et al., 2008). These observations argue against the S3-S4 linker housing a single residue that is a key mediator of gambierol sensitivity.

In the closed state, the pocket that can accommodate gambierol is contoured by the S3b-S4 region, the S4-S5 linker and parts of the S5 and S6 segment. As channel opening involves structural changes within the channel protein, the decrease in gambierol affinity upon channel opening might be caused by a reorientation of gambierol´s binding determinants in the S5 and S6 segment. However, the most striking difference between the closed and open channel

configuration was a conformational change in the shape of the binding pocket. Whereas in the closed state the pocket spans from the S3b-S4 region up to residue T427 in S6, in the open state the pocket is split in two volumes that are no longer connected (Figure 4A-B). This change in pocket shape was accompanied with a reduction in the size and volume of the pocket that contacts residue T427. This difference arises because the closed structure exhibits, according to molecular dynamics simulations, looser VSD to pore domain interactions, thus exhibiting a wider solvent exposed area of the S4S5 cavity to the bulk (Jensen et al., 2012). Thus, these VSD-dependent changes in pocket conformation can explain the different affinity for gambierol of the closed versus the open state (Kopljar et al., 2013). Furthermore, the conformation of this putative gambierol binding pocket was clearly different in the gambierol-insensitive Kv2.1 channel (Figure 4C-D). Most notably, in Kv2.1´s closed state the pocked was not lined by the S3b-S4 paddle region and a passageway between the S3b-S4 region and the pore domain was consequently absent (Figure 4C). The closed state model of the chimeric Kv3_S3b-S4_2.1 channel, which displays a reduced gambierol sensitivity compared to WT Kv3.1, suggested that binding pocket is less likely to be lined by the S3b-S4 paddle region compared to WT Kv3.1 (Figure 4E). Furthermore, the modeling shows a pocket structure that is intermediate in shape between Kv3.1 and Kv2.1. Obviously, the closed and open models are snap-shots of a dynamic process whereby the channel regions are moving; therefore we cannot formally define the exact shape of the binding pocket. Nevertheless, the picture that emerges from this molecular modelling is that the shape of the binding pocket can accommodate gambierol most easily in the closed state of Kv3.1 (high affinity state), and that changes in the shape accompany a reduced affinity (Figures 2 and 4).

In conclusion, the S3-S4a region of the VSD contributes to the sensitivity for gambierol of Kv3.1 channels and most likely Kv channels in general. Although this region might be involved in binding gambierol directly, we propose that the conformation of the VSD defines the structure of gambierol´s binding pocket or controls the accessibility of the binding site. Therefore, the affinity does not depend only on single residues but is also determined by the overall shape of the binding pocket. The proposal that the conformation of the VSD can determine the selectivity of (lipophilic) compounds that bind outside the K^+ pore opens new possibilities in drug design to develop highly selective modulators of Kv channels.

Material and Methods

Molecular biology

All Kv channels used were cloned in a pEGFP-N1 expression vector, which was purchased from Clontech (Palo Alto, CA, USA). Chimaeras were created using the QuikChange Site-Directed Mutagenesis kit (Stratagene, La Jolla, Ca, USA) and mutant primers. Double strand sequencing confirmed the presence of the desired modification and the absence of unwanted mutations. Plasmid DNA was amplified in XL2 blue script cells (Stratagene) and isolated using the GenElute HP plasmid maxiprep kit (Sigma-Aldrich, St Louis, MO, USA).

Electrophysiology

Ltk- cells (mouse fibroblasts, ATCC CLL.1.3) were cultured in DMEM with 10% horse serum and 1% penicillin/streptomycin. Cells were transiently transfected with 15 to 200 ng cDNA for WT channels or chimaeras using polyethyleneimine PEI (Boussif et al., 1995), that was purchased from Sigma-Aldrich. Current measurements were done ~20-28 hours after transfection at room temperature (20-23°C) with an Axopatch-200B amplifier and digitized with a Digidata-1200A (Molecular Devices, Sunnyvale, CA, USA). Command voltages and data storage were controlled with pClamp10 software. Patch pipettes were pulled from 1.2 mm quick-fill borosilicate glass capillaries (World Precision Instruments, Sarasota, FL, USA) with a P-2000 puller (Sutter Instrument Co., Novato, CA, USA) and heat polished. The bath solution contained (in mM) NaCl 130, KCl 4, CaCl2 1.8, MgCl2 1, HEPES 10, Glucose 10, adjusted to pH 7.35 with NaOH. The pipette solution contained (in mM) KCl 110, K4BAPTA 5, K2ATP 5, MgCl2 1, HEPES 10, adjusted to pH 7.2 with KOH. Junction potentials were zeroed with the filled pipette in the bath solution. Experiments were excluded from analysis if the voltage error estimate based on the size of the current exceeded 5 mV after series resistance compensation.

Gambierol (CAS 146763-62-4) was synthesized as described previously (Johnson et al., 2006). Because of its lipophilic character, stock solutions were prepared as 20 µM and 300 µM in DMSO and diluted with the external solution to appropriate concentrations. The final DMSO concentration never exceeded 0.5% and toxin/drug concentrations were applied using a fast perfusion system (ALA scientific, Farmingdale, NY, USA). Flecainide and tetraethylammonium (TEA) were obtained from Meda Pharma (Brussels, Belgium) and Sigma-Aldrich, respectively.

Data analysis

Details of voltage protocols were adjusted based on the different biophysical properties of the channels. The voltage dependence of activation and inactivation were fitted with a single Boltzmann equation: $y = 1/\{1 + \exp[-(V - V_{1/2})/k]\}$, where V represents the applied voltage, $V_{1/2}$ the potential at which 50% of the channels have opened or inactivated, and k the slope factor. Dose-response curves were obtained by plotting y, the fraction of current remaining at +40 mV, as a function of toxin/drug concentration T and fitted with the Hill equation $1-y = 1/(1 + (IC_{50}/[T])^{n}_{H})$, where IC_{50} is the concentration that generates 50% inhibition and n_H the Hill coefficient. Time constants of channel activation were determined by fitting the rise in ionic current activation with a single exponential function. Results are expressed as mean ± SEM with n the number of cells analyzed; error flags are shown if larger than symbol size.

Homology modeling of Kv2.1 and Kv3.1.

Open model of the trans-membrane domain of Kv2.1 and Kv3.1 was generated using a similar approach as previously described for generating a Kv1.5 model (Labro et al., 2008). The initial coordinates for generating the open state models were from the Kv1.2 3D crystal structure (Long et al., 2007), downloaded from the PDB databank (entry code: 2R9R). Sequence alignments were constructed and refined using Muscle 2.6 (Edgar, 2004). A set of 50 different models with a maximum RMSD of 4 Å were generated using the comparative modeling technique as implemented in the Modeller 9.12 package (http://salilab.org/modeller/). The final modeled structures were then optimized to release possible steric clashes due to the newly replaced side-chains, using computational procedures described previously (Labro et al., 2008). Using the same procedure, closed state models of Kv2.1 and Kv3.1 were generated using a theoretical closed model of the Kv1.2 channel as template (Jensen et al., 2012). Figures were generated using the VMD software (Humphrey et al., 1996).

Binding pockets detection and calculate volumes

Detection of pockets and calculation of their volume was performed using the FPOCKET package (Le, V et al., 2009). It is fast and well suited for high throughput pocket detection and construction of cavity databases. The method relies on the Voronoi tesselation and a pocket is detected when a series of spheres contacting neighboring atoms (4 atoms at least) clusters

together and no internal atom is found. Then the ensemble of spheres from the atoms of a protein are filtered according to some minimal and maximal radii values to detect a single cavity.

Acknowledgments

We are grateful to David E. Shaw and Morten Ø. Jensen for providing us the coordinates of their Kv1.2/2.1 closed state channel model. We wish to thanks Oscar Moran for helpful discussions . This work was supported by the 'Vlaams Instituut voor de bevordering van het Wetenschappelijk-Technologisch Onderzoek in de Industrie' (IWT, fellowship to I.K.) and the Belgian Research Fund Flanders (FWO grant G.0433.12N to D.J.S. and J.T.; FWO grant G.0E34.14 to J.T.). J.T. also received funding from the IUAP 7/10 (Inter-University Attraction Poles Program, Belgian State, Belgian Science Policy) and OT/12/081 (KU Leuven).

Reference List

Alabi, A.A., Bahamonde, M.I., Jung, H.J., Kim, J.I., Swartz, K.J., 2007. Portability of paddle motif function and pharmacology in voltage sensors. Nature *450*, 370-375.

Barber, A.F., Liang, Q., Amaral, C., Treptow, W., Covarrubias, M., 2011. Molecular mapping of general anesthetic sites in a voltage-gated ion channel. Biophys. J. *101*, 1613-1622.

Bhattacharji, A., Kaplan, B., Harris, T., Qu, X., Germann, M.W., Covarrubias, M., 2006. The concerted contribution of the S4-S5 linker and the S6 segment to the modulation of a Kv channel by 1-alkanols. Mol. Pharmacol. *70*, 1542-1554.

Birinyi-Strachan, L.C., Gunning, S.J., Lewis, R.J., Nicholson, G.M., 2005. Block of voltage-gated potassium channels by Pacific ciguatoxin-1 contributes to increased neuronal excitability in rat sensory neurons. Toxicol. Appl. Pharmacol. *204*, 175-186.

Blunck, R., Batulan, Z., 2012. Mechanism of electromechanical coupling in voltage-gated potassium channels. Front Pharmacol. *3*, 166.

Borjesson, S.I., Elinder, F., 2011. An electrostatic potassium channel opener targeting the final voltage sensor transition. J. Gen. Physiol *137*, 563-577.

Boussif, O., Lezoualc'h, F., Zanta, M.A., Mergny, M.D., Scherman, D., Demeneix, B., Behr, J.P., 1995. A versatile vector for gene and oligonucleotide transfer into cells in culture and in vivo: polyethylenimine. Proc. Natl. Acad. Sci. U. S. A *92*, 7297-7301.

Cao, Z., Cui, Y., Busse, E., Mehrotra, S., Rainier, J.D., Murray, T.F., 2014. Gambierol inhibition of voltage-gated potassium channels augments spontaneous Ca2+ oscillations in cerebrocortical neurons. J. Pharmacol. Exp. Ther. *350*, 615-623.

Catterall, W.A., Cestele, S., Yarov-Yarovoy, V., Yu, F.H., Konoki, K., Scheuer, T., 2007. Voltage-gated ion channels and gating modifier toxins. Toxicon *49*, 124-141.

Cuypers, E., Abdel-Mottaleb, Y., Kopljar, I., Rainier, J.D., Raes, A.L., Snyders, D.J., Tytgat, J., 2008. Gambierol, a toxin produced by the dinoflagellate *Gambierdiscus toxicus*, is a potent blocker of voltage-gated potassium channels. Toxicon *51*, 974-983.

Delemotte, L., Kasimova, M.A., Klein, M.L., Tarek, M., Carnevale, V., 2015. Free-energy landscape of ion-channel voltage-sensor-domain activation. Proc. Natl. Acad. Sci. U. S. A *112*, 124-129.

Edgar, R.C., 2004. MUSCLE: multiple sequence alignment with high accuracy and high throughput. Nucleic Acids Res. *32*, 1792-1797.

Fuwa, H., Kainuma, N., Tachibana, K., Tsukano, C., Satake, M., Sasaki, M., 2004. Diverted total synthesis and biological evaluation of gambierol analogues: elucidation of crucial structural elements for potent toxicity. Chemistry. *10*, 4894-4909.

Ghiaroni, V., Sasaki, M., Fuwa, H., Rossini, G.P., Scalera, G., Yasumoto, T., Pietra, P., Bigiani, A., 2005. Inhibition of voltage-gated potassium currents by gambierol in mouse taste cells. Toxicol. Sci. *85*, 657-665.

Harris, T., Shahidullah, M., Ellingson, J.S., Covarrubias, M., 2000. General anesthetic action at an internal protein site involving the S4-S5 cytoplasmic loop of a neuronal K(+) channel. J. Biol. Chem. *275*, 4928-4936.

Heginbotham, L., MacKinnon, R., 1992. The aromatic binding site for tetraethylammonium ion on potassium channels. Neuron *8*, 483-491.

Herrera, D., Mamarbachi, A., Simoes, M., Parent, L., Sauve, R., Wang, Z., Nattel, S., 2005. A single residue in the S6 transmembrane domain governs the differential flecainide sensitivity of voltage-gated potassium channels. Mol. Pharmacol. *68*, 305-316.

Hidalgo, J., Liberona, J.L., Molgo, J., Jaimovich, E., 2002. Pacific ciguatoxin-1b effect over Na+ and K+ currents, inositol 1,4,5-triphosphate content and intracellular Ca2+ signals in cultured rat myotubes. Br. J. Pharmacol. *137*, 1055-1062.

Humphrey, W., Dalke, A., Schulten, K., 1996. VMD: visual molecular dynamics. J. Mol. Graph. *14*, 33-38.

Jensen, M.O., Jogini, V., Borhani, D.W., Leffler, A.E., Dror, R.O., Shaw, D.E., 2012. Mechanism of voltage gating in potassium channels. Science *336*, 229-233.

Johnson, H.W., Majumder, U., Rainier, J.D., 2006. Total synthesis of gambierol: subunit coupling and completion. Chemistry. *12*, 1747-1753.

Kopljar, I., Labro, A.J., Cuypers, E., Johnson, H.W., Rainier, J.D., Tytgat, J., Snyders, D.J., 2009. A polyether biotoxin binding site on the lipid-exposed face of the pore domain of Kv channels revealed by the marine toxin gambierol. Proc. Natl. Acad. Sci. U. S. A *106*, 9896-9901.

Kopljar, I., Labro, A.J., de Block, T., Rainier, J.D., Tytgat, J., Snyders, D.J., 2013. The ladder-shaped polyether toxin gambierol anchors the gating machinery of Kv3.1 channels in the resting state. J. Gen. Physiol *141*, 359-369.

Labro, A.J., Grottesi, A., Sansom, M.S., Raes, A.L., Snyders, D.J., 2008. A Kv channel with an altered activation gate sequence displays both "fast" and "slow" activation kinetics. Am. J. Physiol Cell Physiol *294*, C1476-C1484.

Labro, A.J., Snyders, D.J., 2012. Being flexible: the voltage-controllable activation gate of kv channels. Front Pharmacol. *3*, 168.

Le, G., V, Schmidtke, P., Tuffery, P., 2009. Fpocket: an open source platform for ligand pocket detection. BMC. Bioinformatics. *10*, 168.

Lee, S.Y., Banerjee, A., MacKinnon, R., 2009. Two Separate Interfaces between the Voltage Sensor and Pore Are Required for the Function of Voltage-Dependent K^+ Channels. PLoS. Biol. *7*, e47.

Li-Smerin, Y., Swartz, K.J., 2000. Localization and molecular determinants of the Hanatoxin receptors on the voltage-sensing domains of a K(+) channel. J. Gen. Physiol. *115*, 673-684.

Long, S.B., Campbell, E.B., MacKinnon, R., 2005. Crystal structure of a mammalian voltage-dependent *Shaker* family K^+ channel. Science *309*, 897-903.

Long, S.B., Tao, X., Campbell, E.B., MacKinnon, R., 2007. Atomic structure of a voltage-dependent K+ channel in a lipid membrane-like environment. Nature *450*, 376-382.

Lu, Z., Klem, A.M., Ramu, Y., 2002. Coupling between voltage sensors and activation gate in voltage-gated K^+ channels. J. Gen. Physiol *120*, 663-676.

Marzian, S., Stansfeld, P.J., Rapedius, M., Rinne, S., Nematian-Ardestani, E., Abbruzzese, J.L., Steinmeyer, K., Sansom, M.S., Sanguinetti, M.C., Baukrowitz, T., Decher, N., 2013. Side pockets provide the basis for a new mechanism of Kv channel-specific inhibition. Nat. Chem. Biol. *9*, 507-513.

Mattei, C., Marquais, M., Schlumberger, S., Molgo, J., Vernoux, J.P., Lewis, R.J., Benoit, E., 2010. Analysis of Caribbean ciguatoxin-1 effects on frog myelinated axons and the neuromuscular junction. Toxicon *56*, 759-767.

Nicholson, G.M., Lewis, R.J., 2006. Ciguatoxins: Cyclic Polyether Modulators of Voltage-gated ion Channel Function. Marine Drugs *4*, 82-118.

Ottosson, N.E., Liin, S.I., Elinder, F., 2014. Drug-induced ion channel opening tuned by the voltage sensor charge profile. J. Gen. Physiol *143*, 173-182.

Perez, S., Vale, C., Alonso, E., Fuwa, H., Sasaki, M., Konno, Y., Goto, T., Suga, Y., Vieytes, M.R., Botana, L.M., 2012. Effect of gambierol and its tetracyclic and heptacyclic analogues in cultured cerebellar neurons: a structure-activity relationships study. Chem. Res. Toxicol. *25*, 1929-1937.

Phillips, L.R., Milescu, M., Li-Smerin, Y., Mindell, J.A., Kim, J.I., Swartz, K.J., 2005. Voltage-sensor activation with a tarantula toxin as cargo. Nature *436*, 857-860.

Satake, M., Murata, M., Yasumoto, T., 1993. Gambierol - A New Toxic Polyether Compound Isolated from the Marine Dinoflagellate Gambierdiscus-Toxicus. J. Am. Chem. Soc. *115*, 361-362.

Schlumberger, S., Mattei, C., Molgo, J., Benoit, E., 2010a. Dual action of a dinoflagellate-derived precursor of Pacific ciguatoxins (P-CTX-4B) on voltage-dependent K^+ and Na^+ channels of single myelinated axons. Toxicon *56*, 768-775.

Schlumberger, S., Ouanounou, G., Girard, E., Sasaki, M., Fuwa, H., Louzao, M.C., Botana, L.M., Benoit, E., Molgo, J., 2010b. The marine polyether gambierol enhances muscle contraction and blocks a transient K^+ current in skeletal muscle cells. Toxicon *56*, 785-791.

Sigg, D., 2014. Modeling ion channels: past, present, and future. J. Gen. Physiol *144*, 7-26.

Sigg, D., Bezanilla, F., 2003. A physical model of potassium channel activation: from energy landscape to gating kinetics. Biophys. J. *84*, 3703-3716.

Swartz, K.J., 2007. Tarantula toxins interacting with voltage sensors in potassium channels. Toxicon *49*, 213-230.

Swartz, K.J., MacKinnon, R., 1997. Mapping the receptor site for hanatoxin, a gating modifier of voltagedependent K^+ channels. Neuron *18*, 675-682.

Trainer, V.L., Baden, D.G., Catterall, W.A., 1994. Identification of peptide components of the brevetoxin receptor site of rat brain sodium channels. J. Biol. Chem. *269*, 19904-19909.

Trainer, V.L., Thomsen, W.J., Catterall, W.A., Baden, D.G., 1991. Photoaffinity labeling of the brevetoxin receptor on sodium channels in rat brain synaptosomes. Mol. Pharmacol. *40*, 988-994.

Wulff, H., Castle, N.A., Pardo, L.A., 2009. Voltage-gated potassium channels as therapeutic targets. Nat. Rev. Drug Discov. *8*, 982-1001.

Yamaoka, K., Inoue, M., Hirama, M., 2011. A study on mechanisms of toxic actions of ciguatoxins: existence of functional relationship between CTX3C and charged residues of voltage sensors in $Na_v1.4$ sodium channel. Forensic Toxicology *29*, 125-131.

Table 1

Channel	IC_{50} (nM)	$V_{act\ 1/2}$ (mV)	k (mV)	$IC_{50}/IC_{50}^{3.1}$	$\Delta V_{1/2}^{3.1}$ (mV)
Kv3.1	1.2 ± 0.2	23.5 ± 1.0	5.6 ± 0.3	-	-
Kv2.1	>10 000	12.2 ± 1.4	9.5 ± 0.6	>10 000	-11
Kv3.1_EMcoupling_2.1	2.4 ± 0.2	1.1 ± 1.5	5.9 ± 0.2	2.0	-23
Kv3.1_S1-S4_2.1	280 ± 40	34.8 ± 3.0	9.1± 0.4	233	12
Kv3.1_S1-S3a_2.1	1.9 ± 0.2	44.3 ± 2.4	9.1 ± 0.9	1.6	21
Kv3.1_S3b-S4_2.1	143 ± 28	52.0 ± 0.8	9.4 ± 1.1	119	28
Kv2.1 V404T	504 ± 28	28.7 ± 1.5	16.7 ± 1.5	420	5
Kv2.1 V404T_S3b-S4_3.1	900 ± 41	115.6 ± 9.1	31.5 ± 7.0	750	92

Table 1. Overview of the affinity and the biophysical properties of different chimaeras. $V_{act\ 1/2}$ are the midpoint potentials and k the slope factors of the GV curves, respectively. $\Delta V_{1/2}^{3.1}$ are the shifts in the voltage dependence of channel activation compared to WT Kv3.1 ($\Delta V_{1/2}^{3.1}$ = $V_{act\ 1/2}$ of channel - $V_{act\ 1/2}$ of Kv3.1). IC_{50} is the concentration that induces 50% current inhibition and $IC_{50}/IC_{50}^{3.1}$ the fold difference in gambierol affinity of the channel compared to WT Kv3.1.

Figures

Figure 1

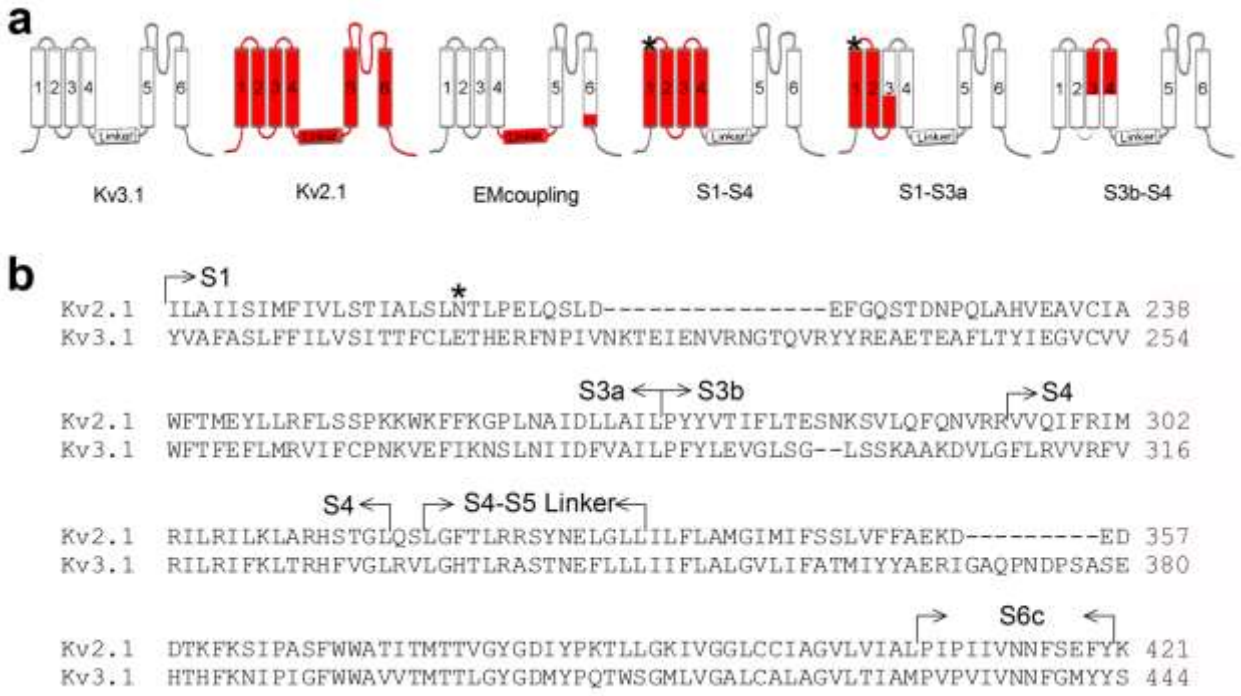

Figure 1. Schematic representation of the chimeric Kv3.1-Kv2.1 channels constructed.
a) Overview of chimaeras between Kv3.1 (white) and Kv2.1 (red). Specific parts of the gating machinery were transplanted from Kv2.1 into Kv3.1, yielding functional channels when expressed in Ltk$^-$ cells. **b**) Sequence alignment of Kv3.1 and Kv2.1 S1-S6 region. Parts that are exchanged are indicated by arrows. Note that the S1-S4 and S1-S3a chimaeras contained an additional Asn to Glu mutation (*) since this residue is crucial for the interaction between S1 and the pore helix (Lee et al., 2009).

Figure 2

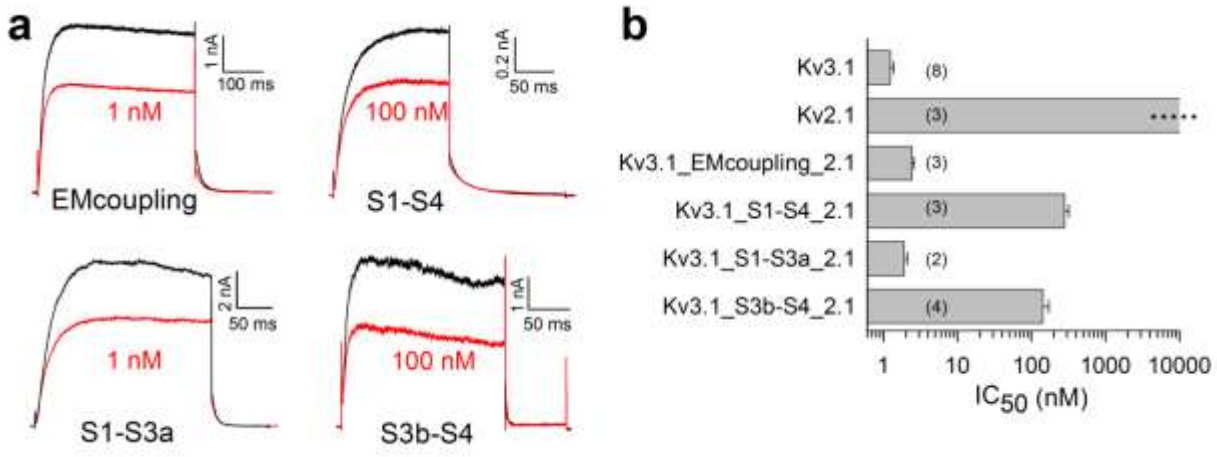

Figure 2. Sensitivity of the different chimeric channels to gambierol inhibition.

a) Current tracings showing the ionic current during a depolarization pulse (EMcoupling: +30 mV, S1-S4: +70 mV, S1-S3a: +60 mV, S3b-S4: + 70 mV) in control and after steady-state inhibition by gambierol. **b**) The IC_{50} values are shown for WT Kv3.1, WT Kv2.1 and the various chimeric channels. Results show that the Kv3.1_S1-S4_2.1 and the Kv3.1_S3b-S4_2.1 chimera displayed a lower affinity for gambierol compared to WT Kv3.1 channels.

Figure 3

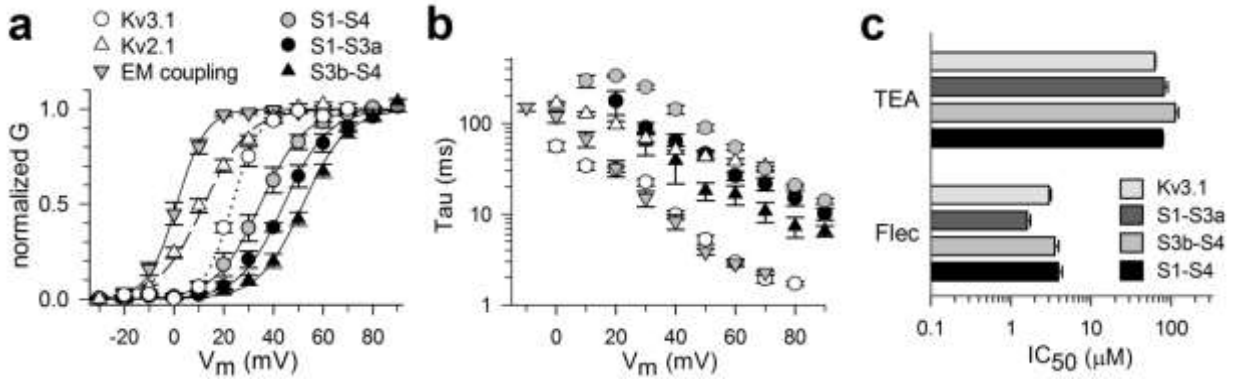

Figure 3. Biophysical properties and TEA/flecainide affinity of the different VSD chimeras.

a) Normalized conductance versus voltage GV relationships which show the voltage dependence of channel activation of WT Kv3.1 (white circles, *n* = 5), WT Kv2.1 (white triangles, *n* = 4) and the different chimeras Kv3.1_EMcoupling_2.1 (gray inverted triangles, *n* = 7), Kv3.1_S1-S4_2.1 (gray circles, *n* = 5), Kv3.1_S1-S3a_2.1 (black circles, *n* = 5), and Kv3.1_S3b-S4_2.1 (black triangles, n = 5). **b**) Time constants of channel activation for WT channels and various chimeras plotted as a function of voltage (meaning of symbols is the same as panel a). **c**) Panel shows for WT Kv3.1 and the different VSD chimeras the IC_{50} value ± S.E.M. of current inhibition by external TEA (top) or Flecainide (bottom). Note that there is no significant difference in the IC_{50} values of the VSD chimaeras compared to WT Kv3.1, which indicates that the VSD chimeras displayed a similar TEA and Flecainide drug sensitivity as WT Kv3.1.

Figure 4

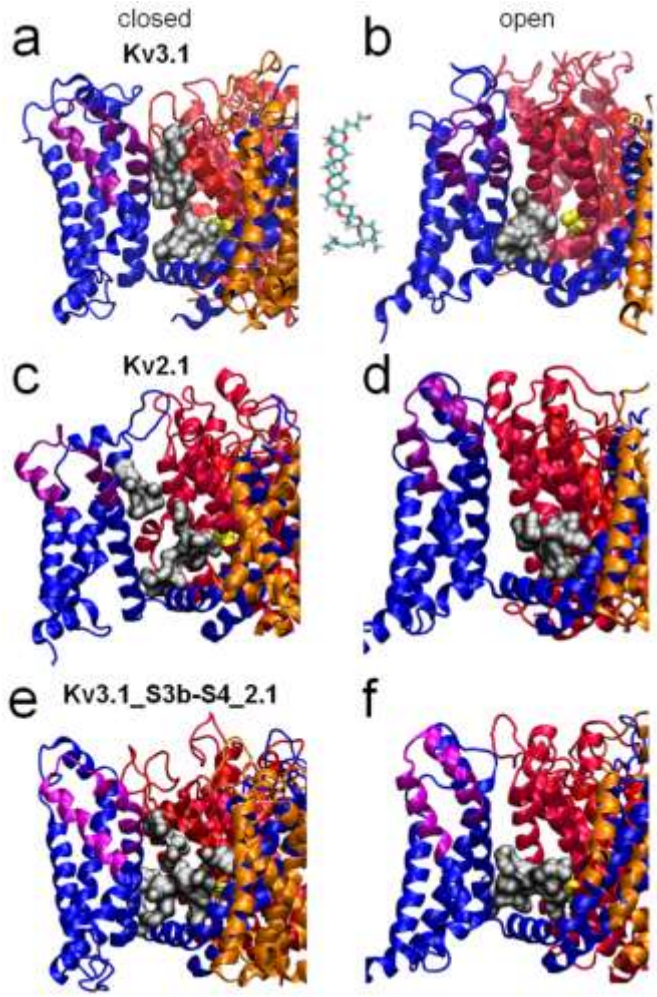

Figure 4. Structure of gambierol´s binding pocket determined by homology modeling.

a-b) Closed (panel **a**) and open (panel **b**) state homology models of Kv3.1 viewed from the side, respectively. Each of the four subunit is represented in a different color (blue, red, pink, and orange respectively). For clarity only the binding pocket that is lined between the S6c residue T427 of the red subunit (yellow residue) and the VSD of the blue subunit is shown (grey volume). The blue subunit´s S3b-S4 paddle region is shown in purple. Note that in Kv3.1´s closed state model (panel **a**) the pocket space (grey volume) stretches from the S3b-S4 region (purple) until residue T427 (yellow) of the red subunit. In Kv3.1´s open state model (panel **b**) the pocket is more confined around S6c. **c-d**) Closed and open state homology models of Kv2.1 viewed from the side with the same color coding as the Kv3.1 models (panel **a-b**). Panel **c** represents 1 of the four pockets of Kv2.1´s closed state model. Although the volume around the S3b-S4 paddle of the blue subunit (purple region) is shown there is no communication with the pocket space that is lined by the S6c residue V404 (yellow) of the red subunit. Panel **d** displays the open state model of Kv2.1. **e-f**) Closed and open conformation models of the chimeric Kv3.1_S3b-S4_2.1 channel as viewed from the side, respectively. Note that in the closed state model (panel **e**) the communication between S3b-S4 paddle and T427 in S6c is reduced compared to Kv3.1´s closed state model (panel **a**). The open state model (panel **f**) shows a picture similar to the open state models of Kv3.1 (panel **b**) and Kv2.1 (panel **d**) with the pocket space confined around S6c.

Supplementary Material

Figure S1

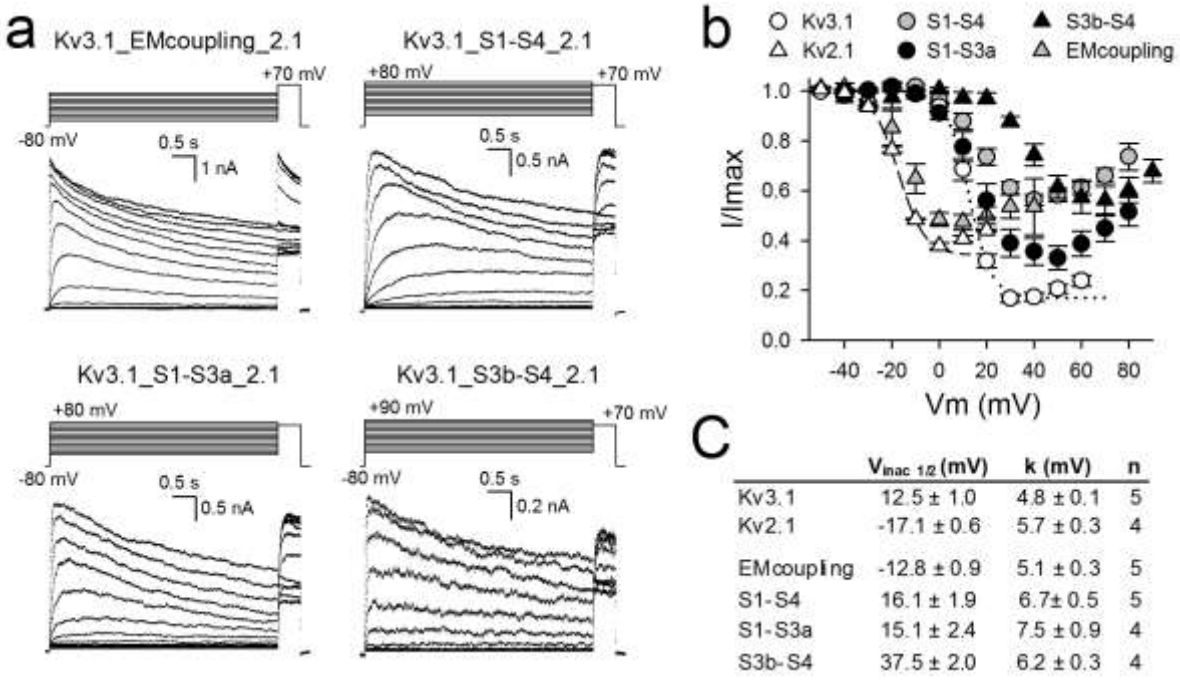

c

	$V_{inac\ 1/2}$ (mV)	k (mV)	n
Kv3.1	12.5 ± 1.0	4.8 ± 0.1	5
Kv2.1	-17.1 ± 0.6	5.7 ± 0.3	4
EMcoupling	-12.8 ± 0.9	5.1 ± 0.3	5
S1-S4	16.1 ± 1.9	6.7± 0.5	5
S1-S3a	15.1 ± 2.4	7.5 ± 0.9	4
S3b-S4	37.5 ± 2.0	6.2 ± 0.3	4

Figure S1. Voltage dependence of inactivation for the chimeric channels.

Panel **a** shows representative ionic current recordings to determine the inactivation process in the chimeras Kv3.1_EMcoupling_2.1, Kv3.1_S1-S4_2.1, Kv3.1_S1-S3a_2.1, and Kv3.1_S3b-S4_2.1 elicited by applying depolarization steps from a -80 mV holding potential (pulse protocols are shown on top and inter-pulse time was 20 s). Note the gradual decrease in current amplitude during the 5 s depolarization step. To estimate the degree of channel inactivation, a +70 mV test pulse was applied after the 5 s depolarization step. Panel **b** displays the voltage dependence of channel inactivation for WT Kv3.1 (white circles and with the dotted line representing the average Boltzmann fit), WT Kv2.1 (white triangles and dashed line), Kv3.1_EMcoupling_2.1 (gray triangles), Kv3.1_S1-S4_2.1 (gray circles), Kv3.1_S1-S3a_2.1 (black circles), and Kv3.1_S3b-S4_2.1 (black triangles). Data were obtained by plotting the normalized current during the +70 mV test pulse as a function of the pre-pulse depolarization potential. Note that all channels displayed a U-type inactivation profile and the amount of channel inactivation is less at stronger depolarizations. Panel **c** lists for the different channels the mean $V_{inac\ ½}$ and slope factor k value ± S.E.M. with n the number of cells analyzed. Parameters were obtained by approximating the voltage dependence of channel inactivation (plots in panel b) with a Boltzmann equation (see material and methods section).

Figure S2

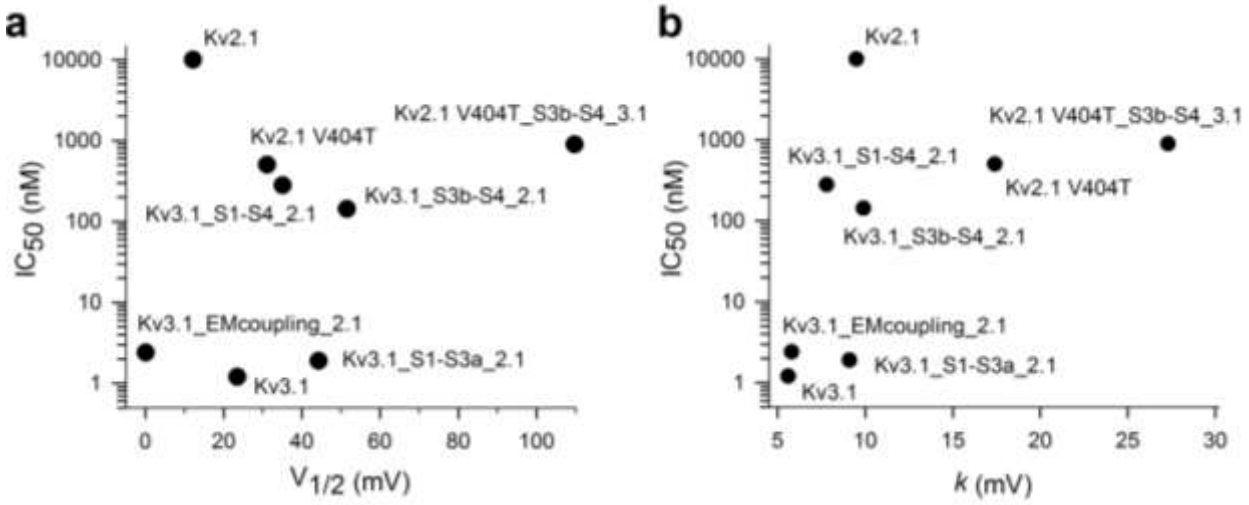

Figure S2. Mapping of the affinity versus biophysical properties.

Graphs display the IC_{50} values of gambierol sensitivity for WT and chimeric channels against either the voltage dependence of channel activation in panel **a** or the slope factor in panel **b**. Both analysis clearly indicated that there is no correlation between both parameters, which suggests that the affinity of the chimeres is not determined by their biophysical properties.

Figure S3

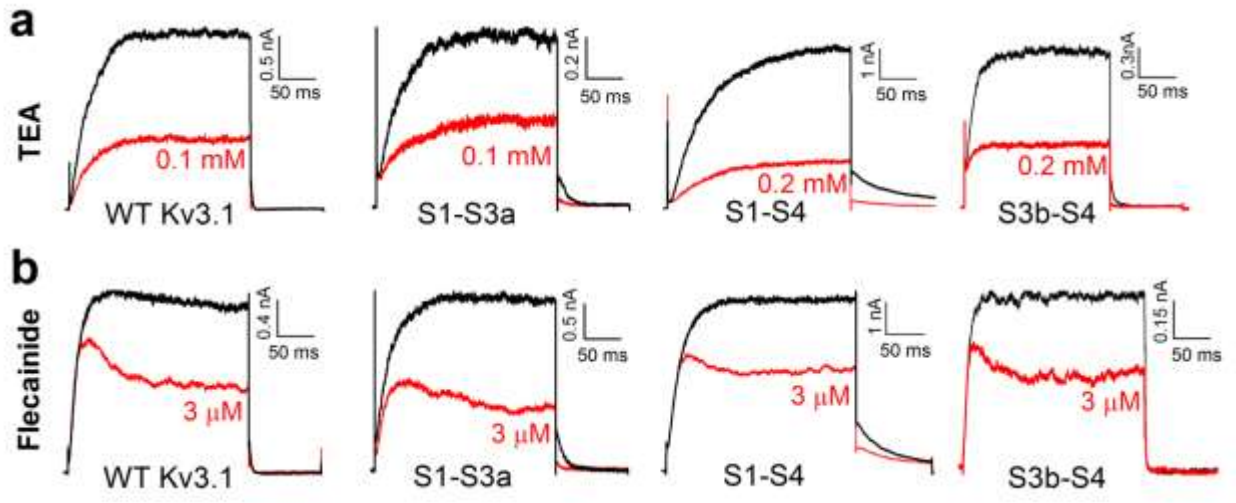

Figure S3. Sensitivity of the different chimeric channels to inhibitors interacting with the pore domain.

a) Current tracings showing the ionic current during a depolarization pulse (WT Kv3.1: +30 mV, S1-S3a: +60 mV, S1-S4: +70 mV, S3b-S4 paddle: + 70 mV) in control (black) and after steady-state inhibition by the external pore blocker TEA (red). **b**) The internal cavity blocker flecainide was tested at depolarization pulses ($V_{1/2}$ + 30 mV) where most of the channels are open. No changes in affinity where observed compared to WT Kv3.1.

Figure S4

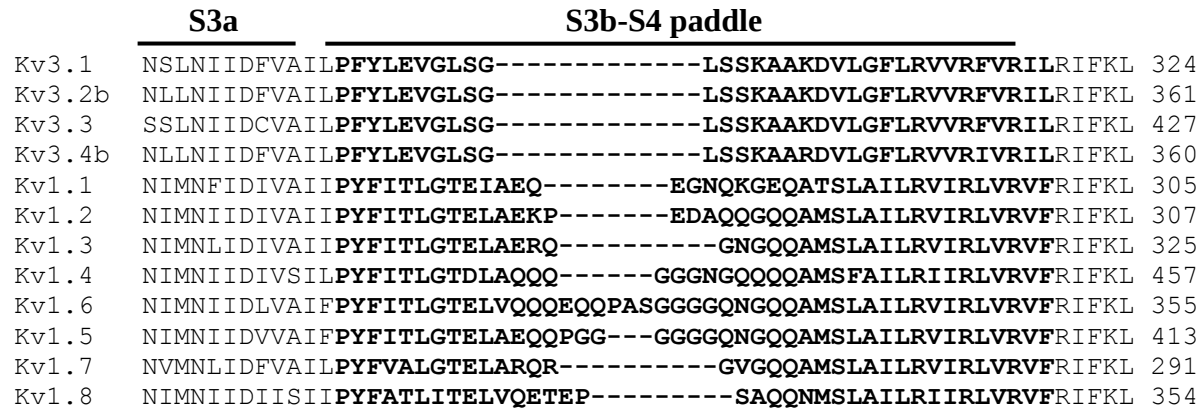

Figure S4. Primary sequence alignment of the S3b-S4 paddle region within Kv3 and Kv1 subfamilies. Whereas the sequence is conserved between Kv3 family members, it is highly variable both in sequence and length between within the Kv1 family.